

Molecular dynamics simulation of large deformation in an amorphous polymer

Ichiro Ogura* and Takashi Yamamoto†

*Department of Physics, Faculty of Science, Yamaguchi University, Yamaguchi 753, Japan
(Received 20 June 1994; revised 7 September 1994)*

Molecular processes in large uniaxial stretching of amorphous polyethylene are studied by molecular dynamics simulation. An initial isotropic amorphous sample nearly free from internal strain is made at 200 K with the aid of Monte Carlo chain generation followed by relaxation of residual strain by the molecular dynamics simulation. The initial sample is cooled to 100 K, and then subjected to a uniaxial stress of 2000 bar. Three independent simulations of uniaxial deformations are made for different draw directions. The system is rapidly elongated at a rate of about $3 \times 10^9 \text{ s}^{-1}$ irrespective of draw direction. The temperature of the system increases markedly during deformation. The temperature rise is very pronounced in the initial stage of deformation, but it slows down markedly around 180 K. Such a change in the rate of temperature rise as well as other anomalies observed in the potential energies of the system are suggested to be closely related to the reported glass transition around $T_g = 180 \text{ K}$. Bond orientation develops continuously by stretching. It is especially conspicuous below 180 K, where the system is considered to be in the glassy state and the molecule does not have sufficient mobility to adjust its conformation to the thermal equilibrium condition. The molecular process of large deformation is found to be divided into three stages: the first stage of breaking interchain binding, probably without serious intrachain deformation; the second stage up to T_g , where a rapid temperature rise occurs accompanied by appreciable void and fibre formation; and the third stage above T_g , where the further development of voids and fibres becomes very conspicuous due to the increased chain mobility.

(Keywords: computer simulation; amorphous polymer; deformation)

INTRODUCTION

Polymers are very important materials in modern technology. Besides their immense potential as functional polymers, their unique mechanical properties and their ease of mechanical processing are a source of much interest. Large macroscopic deformation of polymeric materials is a very important process in fibre formation, fracture, etc. Microscopic understanding of the process is of great benefit both for the control of polymer processing and for the improvement of mechanical properties. The present state of knowledge is, however, very limited; only phenomenological studies of the microscopic response to applied stress have been performed.

Computer simulation is a new branch of polymer science that has grown greatly in the last decade. Realistic simulations of dense polymer systems have become possible owing to the advent of present-day computers¹. Very intensive investigations are being undertaken on various polymer systems, crystals^{2–4}, melts and amorphous polymers^{5,6}, liquid crystals⁷, etc., mostly of their equilibrium properties.

Computer simulation is also very promising in the molecular-level understanding of non-equilibrium

processes. In fact, several investigations are emerging where the potential power of the simulation method is exploited in the studies of polymer deformation and fracture^{8–10}. In this paper, we present a molecular dynamics (MD) simulation of very large deformation in amorphous polyethylene; thereby we hope to demonstrate realistic molecular processes of large deformation and fracture¹¹.

MODEL AND METHOD

The polymethylene chain we consider is made of 512 CH_2 groups, which are treated as united atoms of mass 14 with interaction centres at the carbon atom positions. The united atoms are connected by the usual C–C bonds. The molecule is flexible, having degrees of freedom in bond stretching, bond angle bending and internal rotation. The intramolecular and intermolecular energy parameters used are listed in *Table 1*; the van der Waals interactions are truncated at 2.5σ .

The molecule is placed in an MD cell with the aid of a periodic boundary condition. The initial MD cell before deformation is a cubic one with each dimension being 24 Å; the resulting density is 0.86 g cm^{-3} . The response to an applied uniaxial stress of 2000 bar is simulated up to 120 000 steps (0.5 ns), where the usual numeric integration method of leapfrog is used with a time step of 4.2 fs. Since the deformation rate in the present simulation is very large, $3 \times 10^9 \text{ s}^{-1}$, the whole deformation

* Present address: Department of Organic and Polymeric Materials, Tokyo Institute of Technology, Tokyo 152, Japan

† To whom correspondence should be addressed

process is assumed to be adiabatic and no temperature control is made.

The tensile deformation of the sample is treated by an algorithm, essentially that of Clarke and Brown⁸. The size of the MD cell is changed to adjust the imbalance between the external applied stress and the internal stress calculated by the virial theorem. The deformation rate of the cell is thus given by:

$$\dot{h} = \frac{\sigma - \sigma_0}{M} \quad (1)$$

where the matrix h is made of the basis vectors a, b, c that determine the shape of the MD cell, σ and σ_0 are the internal and external stress tensors, and M is a constant that controls the deformation rate. We consider here only uniaxial tension and ignore the shear stress; the off-diagonal elements of h and σ are taken to be zero. The sample behaves as if it were clamped by slabs at both end surfaces. In order to accelerate macroscopic

deformation, the parameter M is set smaller than that used by Clarke and Brown⁸ (Table 1).

In order to make the initial amorphous sample as isotropic and unstressed as possible, we adopted a procedure devised by Clarke and Brown⁸: a random-coil conformation in the cell was made first by a Monte-Carlo-like random walk through space, then followed by relaxation of the residual strain by MD simulation. We generated more than 500 samples at 200 K, which is just above the glass transition temperature T_g of model polyethylene^{1,2}, and have chosen the best one with respect to the isotropy in the chain orientation. This initial sample was then cooled to 100 K, which is well below T_g , and was subjected to tensile deformation.

RESULTS

We made three independent simulations of the tensile deformation under uniaxial tensions parallel to the X, Y and Z directions, where the initial sample was in the glassy state at 100 K. We present in the following the macroscopic deformation, the temperature rise and the possible glass transition, the changes in the bond orientation, and the overall three-dimensional molecular deformation.

Macroscopic deformation rate

Figure 1 shows the changes in the MD cell dimensions parallel and perpendicular to the draw direction. The rate of deformation parallel to each draw direction is found to be of the order of $3 \times 10^9 \text{ s}^{-1}$: 150% deformation in 0.5 ns. The deformation is very fast even compared with present-day experimental technology. On the contrary, the contractions perpendicular to the draw direction are very small; the perpendicular sizes of the MD cell are kept nearly constant, probably due to much slower rates of structural relaxation in these directions. Such tensile deformation with nearly fixed lateral dimensions inevitably leads to the formation of voids.

Table 1 Intramolecular and intermolecular potentials, and the reduced units of temperature and energy. These parameters are obtained from Roe *et al.*⁶

Two-body potential: $V_2(r) = k_b(r - r_0)^2/2$
 $k_b = 3.46 \times 10^7 \text{ J nm}^{-2} \text{ mol}^{-1}$
 $r_0 = 0.152 \text{ nm}$

Three-body potential: $V_3(\theta) = k_\theta(\cos \theta - \cos \theta_0)^2/2$
 $k_\theta = 5 \times 10^5 \text{ J mol}^{-1}$
 $\cos \theta_0 = -1/3$

Four-body potential: $V_4(\phi) = k_\phi \sum a_n \cos^n \phi$
 $k_\phi = 9000 \text{ J mol}^{-1}$
 $a_0 = 1.0000, a_1 = 1.3100, a_2 = -1.4140,$
 $a_3 = -0.3297, a_4 = 2.8280, a_5 = -3.3943$

van der Waals potential: $V_{\text{vdW}}(r) = 4\epsilon[(\sigma/r)^{12} - (\sigma/r)^6]$
 $\epsilon = 500 \text{ J mol}^{-1}$
 $\sigma = 0.38 \text{ nm}$

Control parameter $M = 2.625 \times 10^6 \text{ Pa s m}^{-1}$
 Reduced unit of energy = ϵ
 Reduced unit of temperature = ϵ/R

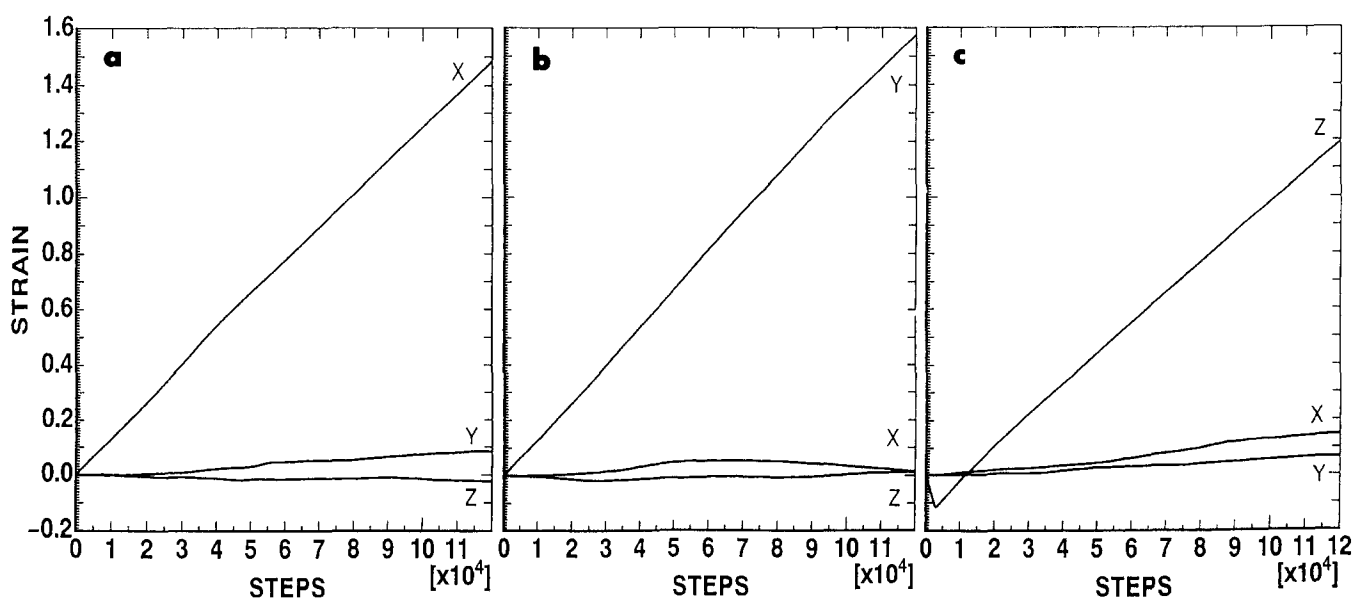


Figure 1 Changes in the MD cell dimensions parallel and perpendicular to the draw direction. The same initial sample is drawn in three directions: (a) in the X axis, (b) in the Y axis, and (c) in the Z axis. Total elongations in 0.5 ns along the draw directions are about 150%

Temperature rise and glass transition

Throughout the stretching process, remarkable temperature increases were noticed. In *Figure 2*, the temperature is plotted as a function of strain; it is seen that the temperature rise is rather independent of the draw direction and is closely correlated to the strain. Temperature rises during adiabatic deformations have been well investigated experimentally in the studies of cold drawing and neck formation. The microscopic origin is, however, not clear. Part of the mechanical work done on the sample will be transferred to kinetic energy, resulting in an increase in temperature. Here we will not elaborate the molecular mechanism of energy transfer; it will be discussed in a separate paper.

It is readily noticed from *Figure 2* that the rate of temperature increase markedly slows down above $\epsilon=0.8$ at 180 K. We should remember here that recent MD simulations^{6,12} showed that the present model of amorphous polyethylene has a glass transition around 200 K. It is therefore reasonable to consider that the marked slow-down of the temperature increase around 180 K observed in our simulation is related to the glass transition. Changes in the potential energies described below also support this view.

During the deformation, the intermolecular and intramolecular potential energies show interesting variations. A typical example is seen in *Figure 3*, where the sample was drawn along the *X* axis. Though the deformation is very rapid, the energies of stretching and angle bending of the C–C bonds are found to show only slight increases; the increases are entirely due to increased thermal energies and are described by $Nk_B T/2$, where N is the number of bonds and k_B is the Boltzmann constant (*Figure 3b*). Below 180 K, however, we can notice a slight deviation from $Nk_B T/2$ in the energy of bond angle bending. It suggests a departure from thermal

equilibrium, below 180 K in the glassy state, in the intramolecular degrees of freedom.

The intermolecular van der Waals energy, on the contrary, shows a fairly rapid increase (*Figure 3c*). The increase in the initial stage of deformation below 180 K is especially remarkable. It is evidently much larger than that expected from thermal energy, and is considered to come from the increasing proximity or separation between chain segments by the forced deformation. Around 180 K the energy suddenly falls off or levels off. The intermolecular strain accumulated during the deformation is considered to be released by the increased chain mobility. This also supports the occurrence of the glass transition around 180 K.

The interpretation of the dihedral angle energy change is, on the other hand, more complicated. The chain elongation will reduce the number of *gauche* bonds and consequently decrease the dihedral angle energy, while the observed temperature rise will increase the energy due to thermal motions. The small energy change observed in *Figure 3d* will be a result of these compensatory effects.

Bond orientation

When an isotropic amorphous polymer is stretched in any direction, chain orientation parallel to that direction will gradually develop. We here introduce the parameters that represent the degrees of bond orientation in the *X*, *Y* and *Z* directions, $\langle b_x^2/b^2 \rangle$, $\langle b_y^2/b^2 \rangle$, $\langle b_z^2/b^2 \rangle$, where \mathbf{b} is the vector connecting next-nearest carbon atoms along the chain, b_x , b_y , b_z are its *x*, *y*, *z* components, and the averages are taken over all \mathbf{b} vectors in the system. In the isotropic state, all these parameters have the same value 1/3.

During the deformation, considerable bond reorientations are observed along the draw direction (*Figure 4*). Below 180 K, where the molecular motions are considered frozen, it seems that the macroscopic deformation directly results in the molecular reorientation, leading to a rapid growth of the bond orientation in the draw direction. Above 180 K, on the other hand, bond orientation develops only gradually. This will be partly because the molecule acquires mobility around T_g and can relax to a less stretched conformation. *Figure 4* shows that the response to the applied stress strongly depends on the draw direction. We believe that such anisotropic response originates from microscopic anisotropies present in the initial amorphous sample, though they are not well characterized at present.

Molecular deformation process in space

The bond orientation parameters discussed above are space-averaged quantities. As will be shown below, the spatial structure in a highly deformed state is very inhomogeneous, and the space-averaged quantities do not always describe the detailed structure faithfully. We therefore monitored the molecular process of deformation in 3D space.

Figure 5 shows the process of elongation along the *X* axis. The initial state is unstretched isotropic amorphous; low-density regions (though very small) are already observable. The onset of deformation results in the growth of microscopic voids, which come to have sizable volumes after 20 000 steps. At 54 000 steps and up to

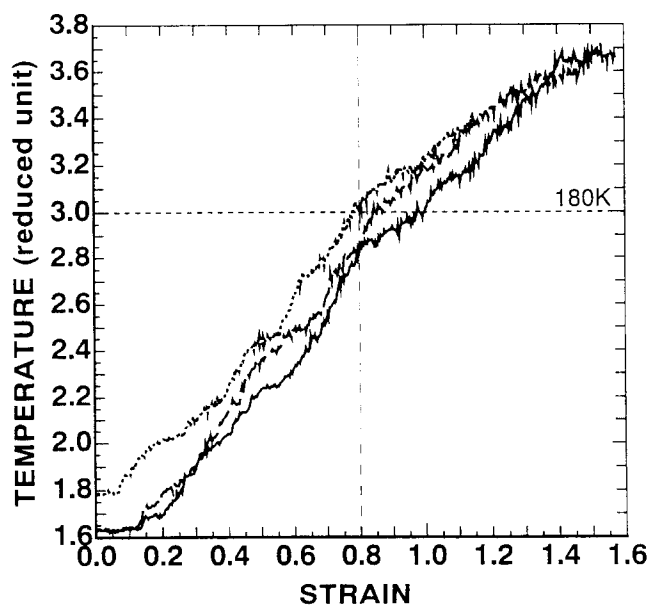


Figure 2 Temperature increases induced by stretching along the *X* axis (full line), the *Y* axis (broken line) and the *Z* axis (dotted line), plotted vs. strain ϵ . The temperature is expressed in reduced unit ϵ/R . Note the difference in slopes below and above $\epsilon=0.8$ (vertical dashed line), which corresponds to about 180 K (horizontal dotted line)

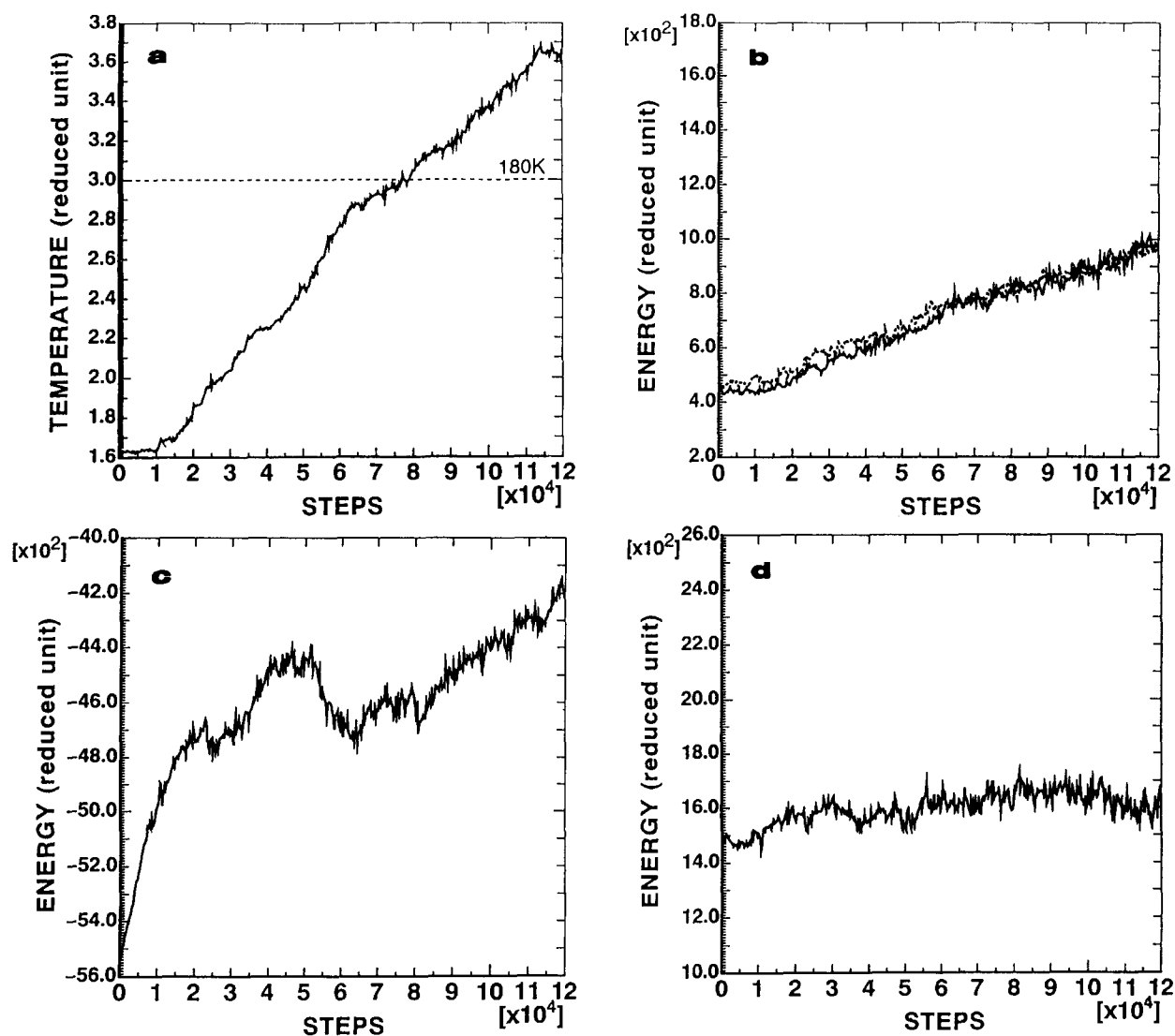


Figure 3 The temperature and the potential energies vs. time during the drawing process along the X axis: (a) temperature, (b) energies in C-C bond stretching (full line) and C-C-C bond angle bending (dotted line), (c) van der Waals energy of interchain interactions, and (d) dihedral angle energy of internal rotation. The energies are expressed in reduced unit ϵ

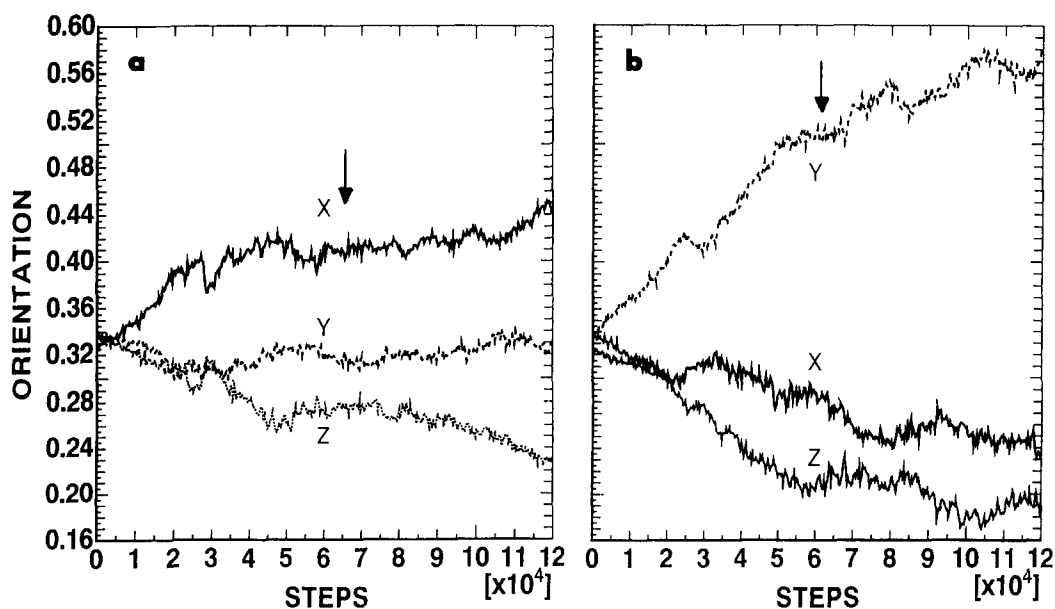


Figure 4 Development of the C-C-C bond orientation during the drawing process along (a) the X axis and (b) the Y axis directions. The bond orientation is expressed by the averaged square of each component of the normalized vector $b/|b|$, where b is the vector connecting the next-nearest carbon atoms. The arrow in each figure represents the assumed glass transition temperature $T_g = 180$ K

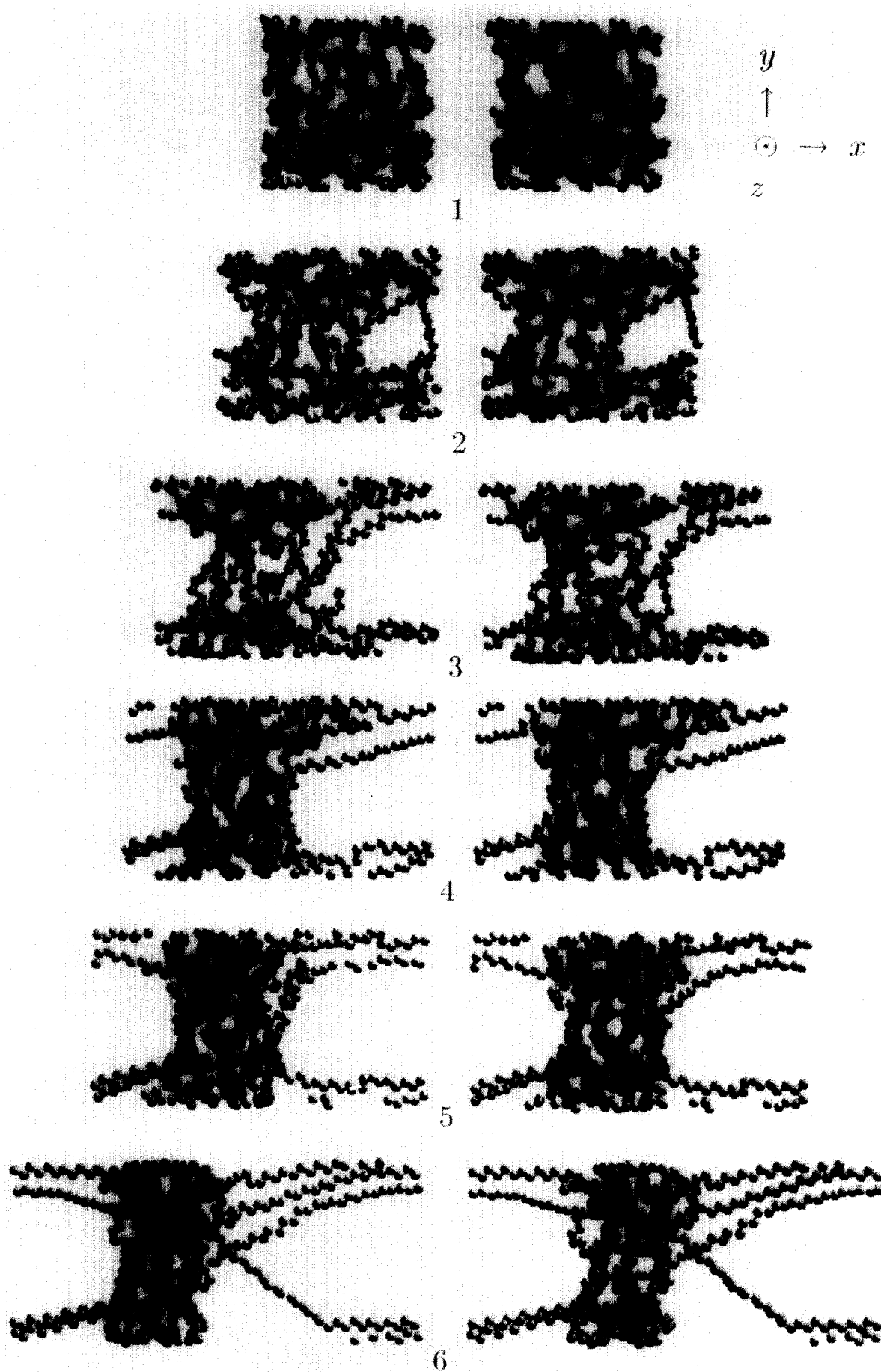


Figure 5 Stereo pictures of molecular deformation process during elongation along the X axis: (1) initial state; (2) at 21 000 steps (80 ps); (3) at 54 000 steps (220 ps); (4) at 65 000 steps (270 ps); (5) at 81 000 steps (330 ps); (6) at 120 000 steps (490 ps)

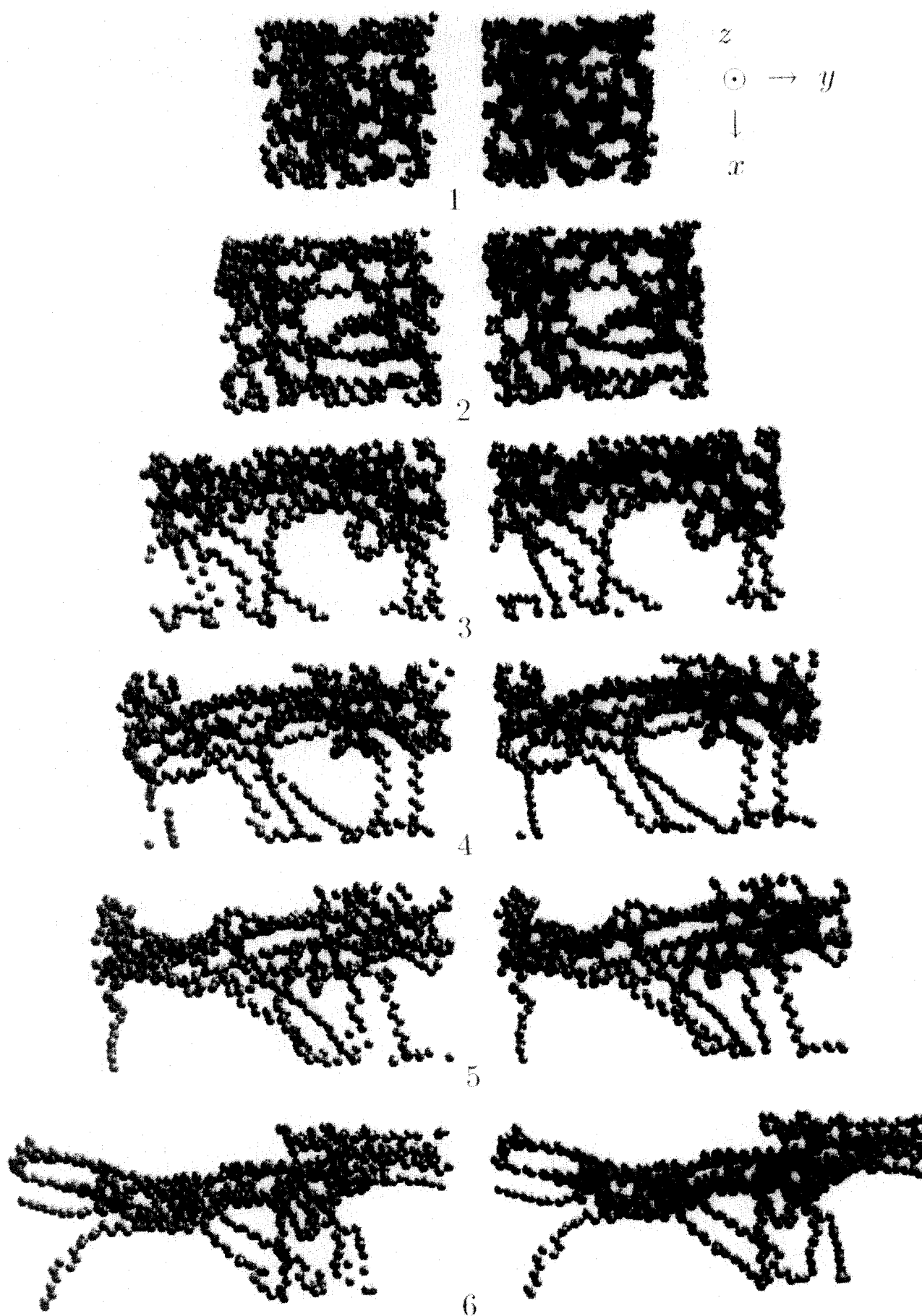


Figure 6 Stereo pictures of molecular deformation process during elongation along the Y axis: (1) initial state; (2) at 21 000 steps (80 ps); (3) at 54 000 steps (220 ps); (4) at 65 000 steps (270 ps); (5) at 81 000 steps (330 ps); (6) at 120 000 steps (490 ps)

180 K, the voids grow continuously. In addition, two distinct regions, oriented fibre-like regions and entangled coil regions, become noticeable. The active molecular motion assumed to set in around 180 K would lead to an appreciable structural relaxation. The most conspicuous one observed here is the shrinkage of the coiled regions and the consequent growth of voids, as is seen at 65 000 steps. Above 180 K the fibre structure grows, further consuming the coiled region.

When the tensile stress is applied in the *Y* direction, our amorphous sample showed quite different behaviour. The chain orientation grew fairly rapidly, leading to a simple fibre formation (Figures 4b and 6). We consider that such a quite anisotropic response to the applied stress originates from the anisotropy in chain entanglement, the difference in the number of chains crossing each MD cell boundary, and also from the local anisotropic order in the chain orientation.

DISCUSSION

Through the process of deformation, we could observe several distinct stages. The initial stage is up to about 40 ps. At this stage, the temperature and the intramolecular energy are kept constant, while the intermolecular energy and the bond orientation grow very rapidly. The segmental packing of the random-coil molecule becomes looser, and the molecule is forced to orient towards the direction of the applied stress without appreciable conformational distortions. From the end of the initial stage till T_g is the second stage, which is characterized by a steep temperature rise. In addition, the intermolecular energy and the bond orientation grow further. A three-phase structure made of voids, coils and fibres becomes noticeable. Above T_g is the third stage. The molecule acquires sufficient mobility and tends to adjust itself to the thermal equilibrium configuration. The molecule reorganizes to reduce intermolecular strain with a consequent growth of voids. The structure of fibres, coils and voids becomes very pronounced.

In the present simulation, the rate of deformation was very large. The purpose of the present paper was to demonstrate a molecular mechanism in very fast deformation processes. The microscopic deformation process is in principle governed by the relative rates of macroscopic deformation and molecular relaxation; both depend strongly on temperature and applied stress. In the present adiabatic deformation, the temperature rise was determined by the deformation rate. Slower deformations under constant-temperature conditions will

evidently lead to quite different microscopic processes. Detailed investigations of the processes under various deformation conditions are the subject of future work.

A large elongation in the draw direction with nearly constant transverse dimensions inevitably leads to void formation reminiscent of crazing. The present MD cell is subjected to a periodic boundary condition, and the extension of Figure 5 by periodic replications gives microcracks and microfibrils. This is qualitatively similar to the usual craze structure. The small MD cell size and the very fast deformation rate, however, inevitably led to an unrealistically small craze dimension. Nevertheless, we consider that the results of our present simulation involve important molecular processes of real deformation.

Since the size of the present system is very small, the results obtained may be infected by many artificial effects. However, the initial formation of voids or fibrils may be triggered by local structural defects like heterogeneous nucleation. The use of a larger MD cell would only increase the probability of the initial events; the microscopic processes especially in the initial stage of deformation are expected not to be much influenced.

It is very impressive that the application of tensile stress in different directions results in quite different molecular modes of deformation. The anisotropy concealed in the initially macroscopically isotropic sample is thought to have a great influence on the detailed deformation process. It will be interesting in future work to clarify and characterize the hidden anisotropy in the chain entanglement, local chain orientation, etc.

REFERENCES

- 1 Roe, R. J. (Ed.) 'Computer Simulation of Polymers', Prentice-Hall, Englewood Cliffs, NJ, 1991
- 2 Yamamoto, T. *J. Chem. Phys.* 1988, **89**, 2356; Yamamoto, T. and Kimikawa, Y. *J. Chem. Phys.* 1992, **97**, 5163; Yamamoto, T., Hikosaka, M. and Takahashi, N. *Macromolecules* 1994, **27**, 1466
- 3 Ryckaert, J. P., Klein, M. L. and MacDonald, I. R. *Mol. Phys.* 1989, **67**, 957
- 4 Sumpter, B. G., Noid, D. W. and Wunderlich, B. *J. Chem. Phys.* 1990, **93**, 6875
- 5 Helfand, E., Wasserman, Z. R. and Weber, T. A. *J. Chem. Phys.* 1979, **70**, 2016
- 6 Takeuchi, H. and Roe, R. J. *J. Chem. Phys.* 1991, **94**, 7458
- 7 Jung, B. and Schurmann, B. L. *Macromolecules* 1989, **22**, 477
- 8 Brown, D. and Clarke, J. H. R. *Macromolecules* 1991, **24**, 2075; *Comput. Phys. Commun.* 1991, **62**, 360
- 9 Blonski, S. and Brostow, W. *J. Chem. Phys.* 1991, **95**, 2890
- 10 Termonia, Y. *Macromolecules* 1989, **22**, 3633
- 11 Ogura, I. and Yamamoto, T. *Kobunshi Ronbunshu* 1994, **51**, 259 (in Japanese)
- 12 Roe, R. J. *J. Chem. Phys.* 1994, **100**, 1610